Vol. 04, No. 2 (2022) 191-202, doi: 10.24874/PES04.02.009

Proceedings on Engineering Sciences

www.pesjournal.net

OPTIMIZATION OF THE MECHANICAL PROPERTIES OF CHEMICALLY ACTIVATED CARBON COMPOSITES IN ORGANIC FRICTION LININGS BY BOX-BEHNKEN DESIGN

Leonard M. Akuwueke,
Chinwuba V. Ossia[1]
Harold U. Nwosu

Received 25.01.2022.
Accepted 04.04.2022.
UDC – 539.92

Keywords:

Activated Carbon; Agro wastes; Mechanical Properties; Box-Behnken design; friction lining; Composites

A B S T R A C T

This study presents the development and physicomechanical optimization of friction lining composites from organic chemically activated carbon. Three types of chemically activated carbon from palm kernel shells (PKS) and coconut shell (CS) giving 3 volumetric ratios of CS (X_{CS}) with 3 particle sizes (X_{PS}) and 3 reinforcement weight concentrations (X_{WT}). The composites were experimentally evaluated for mechanical properties (flexural strength FS, tensile strength TS, hardness H and density D) performance using box-behnken design. ANOVA was used to determine the effects of X_{PS}, X_{CS} and X_{WT}. Results showed that all properties exhibited positive main effects from X_{PS} of order $FS > TS > H > D$, and a positive X_{PS} and X_{CS} interaction. All properties except hardness exhibited negative X_{PS} and X_{WT} , negative X_{WT} and X_{CS}, and positive X_{PS} and X_{CS} interactions. All, except hardness, showed all positive quadratic effect from X_{PS}, X_{WT} and X_{CS}. The experimental and predicted values showed little or no difference. The friction lining composites optimal properties obtained include: hardness $H_{max} = 87.375SD$ at $X_{WT} = 8\%wt, X_{CS} = 100\%CSAC$, $X_{PS} = 60\mu m$; density $D_{min} = 0.97g/cm^3$ at $X_{CS} = 100\%CSAC$, $X_{PS} = 60\mu m$ and $X_{WT} = 4\%wt\, FS_{max} = 39.97696MPa$; at $X_{CS} = 93.33\%CSAC$, $X_{PS} = 150\mu m$, $X_{WT} = 4\%wt$ and $TS_{max} = 28.65MPa$ at $X_{CS} = 100\%CSAC$, $X_{PS} = 150\mu m$, $X_{WT} = 4\%wt$. Hence, all the process variables were relevant for the development of friction-linings using agro-wastes chemically activated carbon.

1. INTRODUCTION

Composite materials have been employed to produce new materials excellent mechanical properties which are suitable for various applications requiring high strength and light weight. Researches have been conducted for the purpose of developing diverse composite materials to evaluate its industrial applications. Pandey et al. (2010) opined that the most widely used natural fibres is plant-based which are derived from the seed, leaf, stalk, wood, bast and fruits of plants whereas, Hughes (2012) opined that fibres obtained from the bast are the strongest and often finds application in automobiles as reinforcement in polymer composites. According to

[1] Corresponding author: Chinwuba Victor Ossia
Email: chinwuba.ossia@uniport.edu.ng

Daryoush and Musbah, (2011) latest research reports of polymer based composite materials have established various approaches for polymer formulations and have permitted the production of innovative products with ideal properties for distinctive application. According to Oladele et al. (2020) the composites can be used as light-weight engineering materials for automobile applications. During the past decade, natural fibre reinforced polymer composites are attaining most convenient applications in sea vehicles, various parts of automotive, medical devices, sporting goods and aerospace industry, due to their classical merits like lesser weight, minimum cost, resistance to corrosion and wear and elevated specific strength etc (Piyush, 2015). Ochola and Mwasiagi (2012) analysed the mechanical properties of natural hybrid fibres reinforced polyester composites according to their weight proportion and length of fibres. Yehia et. al. (1990) developed empirical models for assessing the mechanical properties and morphology of composites prepared by Recycled Low Density PolyEthylene (RLDPE) reinforced with snail shell particles of different weight percentages and sizes. Nuhu and Adeyemi (2015) worked on the development and evaluation of maize husks based brake pad. They observed that hardness, tensile strength, compressive strength increased with a reduction in the filler content. Manikandan et al. (2020) developed models for the prediction of mechanical properties of natural fibres reinforced polymer composites using cotton shell fibres (CSF). They studied the effects of cotton shell particles reinforced composites as a function of CSF particles loading and size. They confirmed that with increase in fibre content and the reduction in fibre size, mechanical properties such as tensile strength, flexural strength and hardness increased. Ruzaidi et al. (2012) studied the mechanical properties (hardness, compressive strength) and wear behaviour of brake pads produced from palm slag. Singh (2015) investigated the influence of mineral fibrous reinforcement like lapinus fibre and wollastonite fibre on the physical, mechanical and wear performance of friction materials. In the conclusion of Singh (2015) the physical and mechanical properties of formulation were found to be well aligned with standard industrial norm. Athijayamani et al. (2010) stated that to predict the response parameters, an empirical, statistical method and theoretical or analytical methods must be followed in general. Maniya and Bhatt (2016) conducted a study to develop a statistical method for evaluating the value of cotton using High Volume Instrument (HVI) to calculate cotton fibre properties. Prediction of surface roughness in drilling of Glass Fiber Reinforced Polymer (GFRP) composite materials has been performed using fuzzy logic rule–based modelling and ANOVA (Latha & Senthilkumar, 2010). Manickam et al. (2015) studied experimentally the mechanical performance of Roselle Fiber-Reinforced Vinyl Ester (RFRVE) composites and thereafter, studied the optimization of process variables in accordance with mechanical properties of RFRVE composite using the grey based-Taguchi method. In the study of Mustafa and Huseyin (2006) where they used the multiple linear regression analysis, the yarn parameters of ring spun cotton yarns were predicted and confirmed that yarn properties were affected by fiber properties, number of yarns, twist and roving properties. The mechanical behaviour of the plain and woven fabric reinforced composites was examined by Hakan and Bulent (2017) and their reports revealed that the weaving arrangement influences the tensile and impact properties of the composites. The optimization of the mechanical properties of chemically activated carbon composites in organic friction linings by Box Behnken design (BBD) have not yet been performed as per the above stated literature review. The objective of the present study is to optimize the mechanical properties of the epoxy composites reinforced with chemically activated carbon reinforcement extracted from agro waste materials such as palm kernel shell and coconut shell respectively as friction lining composite. The required mechanical tests are conducted as per ASTM standards. Also, in this investigation, statistical models were established to predict the mechanical properties of the composites using BBD.

2. MATERIALS AND METHODS

2.1 Materials / Equipment

Materials used in the production of the activated carbon includes Palm Kernel Shell (PKS), Coconut Shell (CS), Calcium Chloride, Distilled water, Volumetric Flask, Measuring Scale, Heat source, Aluminium pot with lid, Ramming mass (castable), Small ceramic pot with laboratory mortar, Ball milling machine and a Timer. The basic materials types used in the production of the lining composites include: activated carbon from palm kernel shells and Coconut shells (PKSAC, 50:50 PKSAC/CSAC mix, CSAC), epoxy Resin *(Epochem 105)*, epoxy hardener / catalyst *(Epochem 205)* and the mould made from Beeswax (Figure 1).

Figure 1. Base Materials, Resin, hardener and mold materials used.

2.2 Methods

(i) Production of Activated Carbon

The Palm kernel shells were bought from a local oil palm processing factory in Orlu, Imo State, Nigeria. The palm kernel shells were then washed, and non-shell materials were carefully removed. The shells were then dried by heating in batches for 30min per batch until the required quantities were obtained. First, the weight of the empty aluminium pot with lid was measured to be 1.2kg. The pot was filled but not to the brim with PKS samples, and the weight of the aluminium pot with lid and the shells was measured to be 6.2kg after sealing the lid on the pot with ramming mass (castable).Therefore, the total weight of the PKS samples was 5kg (6.2 – 1.2kg). An ϕ8mm hole was then drilled on the lid to enable escape of fumes during pyrolysis. Note that the gas pressure from inside was higher than the atmospheric pressure so there was no entrance of oxygen into the heating chamber during pyrolysis. The heat source was activated and the sealed pot containing the PKS materials was then placed on the heater. Heating was monitored for about 4h until no fumes emerged from the drilled hole on the lid. A thermocouple was installed into the aluminium pot via the drilled hole. First, the ambient temperature was measured to be 34^{o}C. The start-up temperature was measure with the thermocouple to be 81^{o}C. Also, at the peak of the fume, the temperature was measured to be 260^{o}C. This was the temperature at which the quantity and pressure of the fumes were high. Finally, the temperature was measured with the same thermocouple when the fumes started diminishing at 265^{o}C. At this point, the gas supply from the cylinder was shut off and the pyrolysis ended. The content was then allowed to cool to room temperature and the weight of the aluminium pot and charred PKS samples was measured to be 3kg. The ramming mass was removed, and the weight of the lid measured to be 0.2kg. The weight of the charred PKS samples was calculated by subtracting the weight of the empty pot with lid from the total weight of the aluminium pot with charred PKS samples which was measured to be 3kg(3 – 1.2 = 1.8kg). Therefore, 1.8kg of charred PKS samples was produced at first pyrolysis. After unsealing the lid and measurements, the charred PKS was removed from the pot. The charred PKS materials were then washed in running water and spread in the open for sun drying for 4 days. The charred PKS materials were then grinded in ball mill to get the required granule size. The processes were repeated to produce more quantities of the charred PKS samples. To produce the activated carbon after pyrolysis$CaCl_2$ was mixed with distilled water in a ratio of 1:3. 100g of $CaCl_2$ was mixed with 300ml of distilled water into a volumetric flask and was stirred to form a solution. The PKS granules were mixed with the $CaCl_2$ solution on a ratio of 2:1. This implied that 300g of PKS was mixed in a solution of 150ml. The mixture was stirred until a paste like material was formed. The paste like material was covered and allowed for 24h. Water was drained from the sample as much as possible and the sample was transferred into an aluminium pot with lid and was heated for 3h to activate. The processes were repeated to produce more quantities of PKS activated carbon.

Coconuts were bought from a local market in Orlu, Imo State, Nigeria. The nuts were broken to separate the shells, after which the shells were broken further into small sizes, washed and non-shell materials were carefully removed. The shells were then sun dried for 7 days. First, the weight of the empty aluminium pot with lid was measured to be 1.2kg. The pot was filled but not to the brim with CS samples, and the weight of the aluminium pot with lid and the shells was measured to be 6.2kg after sealing the lid on the pot with ramming mass (castable). Therefore, the total weight of the CS samples was 5kg (6.2 – 1.2kg). An 8mm diameter hole was then drilled on the lid to enable escape of fumes during pyrolysis. Note that the gas pressure from inside was higher than the atmospheric pressure so there was no entrance of oxygen into the heating chamber during pyrolysis. The heat source was activated and the sealed pot containing the CS materials was then placed on the heater. Heating was monitored for about 3h until no fumes emerge from the drilled hole on the lid. A thermocouple was installed into the aluminium pot through the drilled hole. First, the ambient temperature was measured to be 34^{o}C. The start-up temperature was measure to be 80^{o}C. Also, at the peak of the fume, the temperature was measured to be 260^{o}C. This was the temperature at which the quantity and pressure of the fumes were high. Finally, the temperature was recorded from the same thermocouple when the fumes started diminishing to be 265^{o}C. At this point, the gas supply from the cylinder was shut off and the pyrolysis ended. The content was then allowed to cool to room temperature and the weight of the aluminium pot and charred CS samples was measured to be 2.9kg. The ramming mass was removed, and the weight of the lid measured to be 0.2kg. The weight of the charred CS samples was calculated by subtracting the weight of the empty pot with lid from the total weight of the aluminium pot with charred CS samples which was measured to be 2.9kg (2.9 – 1.2 = 1.7kg). Therefore, 1.7kg of charred CS samples was produced at first pyrolysis. After unsealing the lid and measurements, the content (charred CS) was removed from the pot. The charred CS materials were then washed in running water and spread in the open for sun drying for 4 days. The charred CS materials were then grinded in ball mill to get the required granule size. The processes were repeated to produce more quantities of the charred CS samples. To produce the activated carbon after pyrolysis, $CaCl_2$ was mixed with distilled water in a ratio of 1:3. 100g of $CaCl_2$ was mixed with 300ml of distilled water into a volumetric flask and was stirred to form a solution. The CS granules were mixed with the $CaCl_2$ solution on a ratio of 2:1. This implied that 300g of CS was mixed in a solution of 150ml. The mixture

was stirred until a paste like material was formed. The paste like material was covered and allowed for 24h. Water was drained from the sample as much as possible and the sample was transferred into an aluminium pot with lid and was heated for 3h to activate. The processes were repeated to produce more quantities of the CS activated carbon. The activated carbons thus obtained are shown in Figure 2.

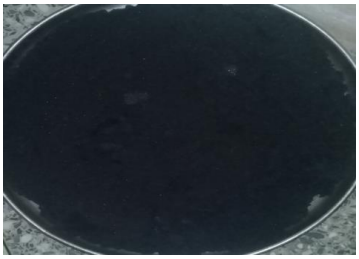

(a)

(b)

Figure 2. Activated Carbons from (a) palm kernel shells (PKSAC) and (b) coconut shells (CSAC)

(ii) Friction lining composite samples fabrication

There are 3 types of reinforcement materials used in the sample preparation namely palm kernel shell activated carbon (PKSAC), Coconut shell activated carbon (CSAC) and 50:50 PKSAC/CSAC volumetric mix. Friction lining composites samples were prepared using these 3 types of reinforcement materials with 3 particle sizes (X_{PS} = 60, 105, 150µm) at 3 different reinforcement weights (X_W = 4, 6, 8%wt) to determine the effect these parameters on the mechanical properties of the samples. Standard volume of sample was chosen to be 10ml. The sample composition was calculated. For 60µm, 96% of the resin + catalyst for 2:1 ratio gave 6.4ml and 3.2ml of resin and catalyst respectively yielding a total of 9.6ml, while 4 wt % of the reinforcement gave 0.4ml. To determine the weight of each 4% reinforcement material, the mass was calculated by multiplying the volume by the densities of the various 60µm of the 3 types of reinforcement materials (PKSAC, CSAC and 50:50 PKSAC/CSAC mix).The process was repeated for the other particle sizes of the other base materials. The detailed composition of the various activated carbon epoxy composites are shown in Table 1.Beeswax casting method was used to produce the specimens. Moulds were then prepared on beeswax before casting. To determine the curing period, a representative sample was prepared and used to measure the hardness on daily basis until hardness value stabilizes. At the end of this testing period, a total of 5 days was expended to have the hardness stabilize. This was used as the basis for setting a curing time of 5days for rest test samples at room temperature, humidity and pressure. Then the cast sample was removed after curing, cleaned, cut and machined to respective sample shapes and dimensions for mechanical tests (tensile, flexural and hardness tests) following relevant ASTM standards. The samples were then prepared for tensile, flexural and shore D hardness test. This was repeated for each sample according to reinforcement weight (X_{RW}) and particle size (X_{PS}) and type of activated carbon concentration (X_{CS}) as base materials. The epoxy / hardener volumetric ratio used in all the composites fabrication was 2:1 in 10ml total volume.

Table 1. Composition of reinforcement, resin and hardener (catalyst) in different composites

Particle Size, µm	Reinforcement Type						X_{RW} (%wt)	Resin + Catalyst (hardener) (%wt)
	PKSAC		PKSAC/CSAC		CSAC			
	Density, (g/ml)	Weight (mg)	Density, (g/ml)	Weight (mg)	Density, (g/ml)	Weight (mg)		
60	0.541	216	0.553	221	0.538	215	4	96
		324		332		322	6	94
		433		442		430	8	92
105	0.530	212	0.533	213	0.520	208	4	96
		318		320		312	6	94
		424		426		416	8	92
150	0.605	242	0.603	241	0.558	223	4	96
		363		362		335	6	94
		484		482		446	8	92

(iii) Testing design of friction lining composites

All friction linings matrix were developed by mixing different types of activated carbon particles (X_{CSAC} = 0%CSAC:100%PKSAC, 50%CSAC:50%PKSAC, 100%CSAC: 0%PKSAC) of particles sizes (X_{ps} = 60, 105, 150µm) to form different reinforcement weights (X_w = 4, 6, 8%wt) with epoxy resin and hardener to obtain a composite matrix. The composition of the various composite friction lining materials derived from chemically activated carbons of PKS and CS agro-wastes, epoxy resin and hardener (catalyst) are shown in Table 1. In this study of the mechanical properties of chemically activated carbon from agro-waste materials reinforced with epoxy composites, a response surface methodology using a 3-factors 3-levels BBD was adopted for the properties optimization. These independent variable settings were considered based on a preliminary study. Analysis of variance (ANOVA)

and data-regression using Microsoft Excel were carried out to identify the relationship between the dependent and independent variables and verify the statistical model. The response surfaces were plotted using sigma plot software.

Table 2. Reinforcement parameters and levels

Reinforcement Parameter (Units)		Factor Levels		
		Low (-1)	Medium (0)	High (+1)
Particle factor X_1	Particle size X_{PS}(μm)	60	105	150
Weight factor, X_2	Reinforcement weight X_{RW}(%wt)	4	6	8
AC type factor, X_3	CSAC concentration X_{CS} (% vol)	0	50	100

The influence of these three parameters on the mechanical properties can be approximated by the following second-order multivariate polynomial model equation (1).

$$Y = \beta_o + \sum_{i=1}^{3} \beta_i X_i + \sum_{i \neq j=1}^{3} \beta_{ij} X_i X_j + \sum_{k=1}^{3} \beta_{kk} {X_k}^2 + e \quad (1)$$

where Y is the predicted mechanical property outcome (tensile strength, flexural strength, hardness, and density), β_o is the model constant, β_i is the linear (main) coefficient, β_{kk} is the quadratic coefficients, β_{ij} is the interaction coefficient, X_i is the coded or normalised independent variables, and e is the experimental error.

The coding equations relating the independent variables with the normalised factors are given in equation (2), (3), and (4) for reinforcement particle factor X_1, weight factor X_2 and type factor X_3 as functions of reinforcement particle size X_{PS}, reinforcement weight X_{RW} and coconut shell activated carbon (CSAC) concentration (X_{CS}), respectively as independent variables.

$$X_1 = \frac{X_{PS}-105}{45} \quad (2)$$

$$X_2 = \frac{X_{RW}-6}{2} \quad (3)$$

$$X_3 = \frac{X_{CS}-50}{50} \quad (4)$$

3. RESULTS AND DISCUSSION

3.1 Experimental output results

Table 3 shows the BBD values and results obtained from the experimental runs. The mechanical properties values obtained were 10.37 ≤ TS ≤ 24.85MPa, 20.58 ≤ FS ≤ 44.38MPa, 60 ≤ H ≤ 81SD, and 0.84 ≤ D ≤ 1.03g/cm3 range for tensile strength (TS), flexural strength (FS), hardness (H) and density (D), respectively.

Table 3. BBD experimental runs parameters for different composites

Runs	Experimental parameters						
	Reinforcement Input parameters combination			Composite Output (Mechanical) properties			
	Particle size (μm)	Reinforcement weight (%wt)	CSAC conc. (% vol)	Tensile strength, MPa	Flexural strength, MPa	Hardness, (Shore D)	Density, (g/cm^3)
1	60	4	50	19.12	28.21	75.5	1.01
2	150	4	50	24.85	41.63	72.0	1.01
3	60	8	50	10.64	32.43	77.0	0.88
4	150	8	50	12.86	32.27	79.0	0.84
5	60	6	100	17.19	35.33	80.0	0.84
6	150	6	100	21.66	40.14	77.0	0.92
7	60	6	0	20.15	44.38	69.0	0.96
8	150	6	0	18.82	43.0	81.0	0.93
9	105	4	100	20.64	32.36	76.0	1.03
10	105	8	100	15.45	31.26	73.0	0.89
11	105	4	0	10.37	20.58	65.0	1.02
12	105	8	0	22.87	36.50	74.5	0.91
13	105	6	50	16.6	43.58	60.0	0.91
14	105	6	50	16.6	43.58	60.0	0.91
15	105	6	50	16.6	43.58	60.0	0.91

3.2 Response Models Process Parameters

(i) Regression and analysis of variance (ANOVA)

The second order multivariate model in Equation (1) is fitted to the experiment results in Table 3 to obtain the models in Table 4. The coefficient of determination (R^2 value) obtained for tensile strength, flexural strength, hardness and density are 0.5938, 0.85012, 0.98042 and 0.94189, respectively. Recall that the R^2 value is a measure of the closeness between experimental and predicted data. Apart from the tensile strength model which exhibited a weak R^2-value, the other R^2-values showed less deviation from actual data. This implies that the models (flexural, hardness and density models) could be used to predict the response within the range of parameters investigated and thus indicates a good fitness of models. Hence, models are capable of explaining 59%, 85%, 98% and 94.2% of the variation for tensile strength, flexural strength, hardness and density responses, respectively. The significance F (column 6 of Table 4) from the analyses of variance (ANOVA) indicates the probability that the model is wrong. The smaller the significance F value the better the model. Hence, the TS-model showed the worst significance F value (0.6304), followed by flexural strength (FS) (0.10959), density (D) (0.01308), and hardness (H) (0.00095). These imply that the TS-model obtained is not very strong as compared to hardness (H) and density D-model.

Table 4. Physico-mechanical property response surface models

s/Nos	Parameter	Model	R^2-value	Standard error	Signif F.
1	Density	$y = 0.91 + 0.00125X_1 - 0.06875X_2 - 0.0175X_3 - 0.01X_1X_2 - 0.0075X_2X_3 + 0.0275X_1X_3 - 0.0125{X_1}^2 + 0.0375{X_2}^2 + 0.015{X_3}^2$	0.94189	0.0250	0.01308
2	Hardness	$y = 60 + 0.9375X_1 + 1.875X_2 + 2.0625X_3 + 1.375X_1X_2 - 3.125X_2X_3 - 3.75X_1X_3 + 10.25{X_1}^2 + 5.625{X_2}^2 + 6.5{X_3}^2$	0.980424	1.7357	0.00095
3	Flexural strength	$y = 43.58 + 2.08625X_1 + 1.21X_2 - 0.67125X_3 - 3.395X_1X_2 - 4.255X_2X_3 + 1.5475X_1X_3 + 0.29625{X_1}^2 - 10.2413{X_2}^2 - 3.16375{X_3}^2$	0.850123	4.5701	0.10959
4	Tensile strength	$y = 16.6 + 1.38625X_1 - 1.645X_2 + 0.34125X_3 - 0.8775X_1X_2 - 4.4225X_2X_3 + 1.45X_1X_3 + 1.195{X_1}^2 - 0.9275{X_2}^2 + 1.66{X_3}^2$	0.593808	4.4824	0.63042

It can be observed that all the properties showed positive main effects with respect to particle size X_{PS} in the order FS > TS > H > D. Density, D and tensile strength, TS showed negative main effect while hardness H and FS showed positive main effect with respect to reinforcement weight concentration X_W. However, density D and flexural strength FS showed negative main effects while hardness and tensile strength TS showed positive main effect with respect to activated carbon type concentration X_{CS} (%vol). A negative main effect means that the property will increase with increase in the independent factor and vice versa.

All the properties except hardness exhibited a negative particle size X_{PS} and reinforcement weight X_{WT} interaction, negative weight X_{WT} and carbon type concentration X_{CS} interaction, and a positive X_{PS} and X_{CS} interaction. This implies that all the properties showed a positive X_{PS} and X_{CS} interaction. Hardness of all samples showed a positive instead of a negative X_{PS} and X_{WT} interaction. A negative interaction effect showed that an increase in one factor was associated with a decrease in the second factor and vice versa. All the properties measured, except hardness, showed all positive quadratic effect with respect to X_{PS}, X_{WT} and X_{CS} accounting for the concave shape of the hardness response surfaces unlike other response surfaces in section 3.3. An all negative quadratic effects would have exhibited dome-shaped (convex) response surfaces.

(ii) p-value Analysis

A p-value less than 0.05 (typically ≤ 0.05) is statistically significant. Therefore, the independent variables with p-values less than 0.05 indicate that the terms of the model significantly affected the response in the design space. From Table 5, the tensile strength model has p-values of main effects (independent variables) exceeding 0.1000 indicate that the model terms were insignificant. Also, for the flexural strength model, (X_2^2) variable is a significant model term with the p-value less than 0.05. In general, hardness and density models showed better significance than those of tensile strength and flexural strength for (X_2) (X_3), (X_2X_3), (X_1 X_3,), (X_1^2), (X_2^2), and (X_3^2) variables.

Table 5. p-values of physicomechanical property models

Source	p-value			
	Tensile Strength	Flexural Strength	Hardness (Shore D)	Density
Intercept	0.0013	0.000014	0.0000000245	0.000000019
X_1	0.4217	0.2531	0.1871	0.8930
X_2	0.3468	0.4876	0.0282	0.0005
X_3	0.8380	0.6950	0.0200	0.1045
X_1X_2	0.7115	0.1974	0.1739	0.4600
X_2X_3	0.1054	0.1216	0.0155	0.5746
X_1X_3	0.5461	0.5283	0.0075	0.0790
X_1^2	0.6302	0.9057	0.00009	0.3807
X_2^2	0.7073	0.0076	0.0015	0.0344
X_3^2	0.5085	0.2408	0.0008	0.3010

(iii) Experimental and predicted property values

The results of the physico-mechanical properties obtained from the conducted experiments and those estimated from the BBD response model equations are shown in Figure 3 for: (a) tensile strength, (b) flexural, (c) hardness, and (d) density respectively. It can be observed that there is not much variation among the experimental values and the predicted values obtained from BBD response models.

It can be observed from Figure 3 that there is negligible variation between the experimental and predicted values of the properties measured. The models for tensile and flexural strengths of samples showed slight but negligible difference, while that of hardness and density show no variations.

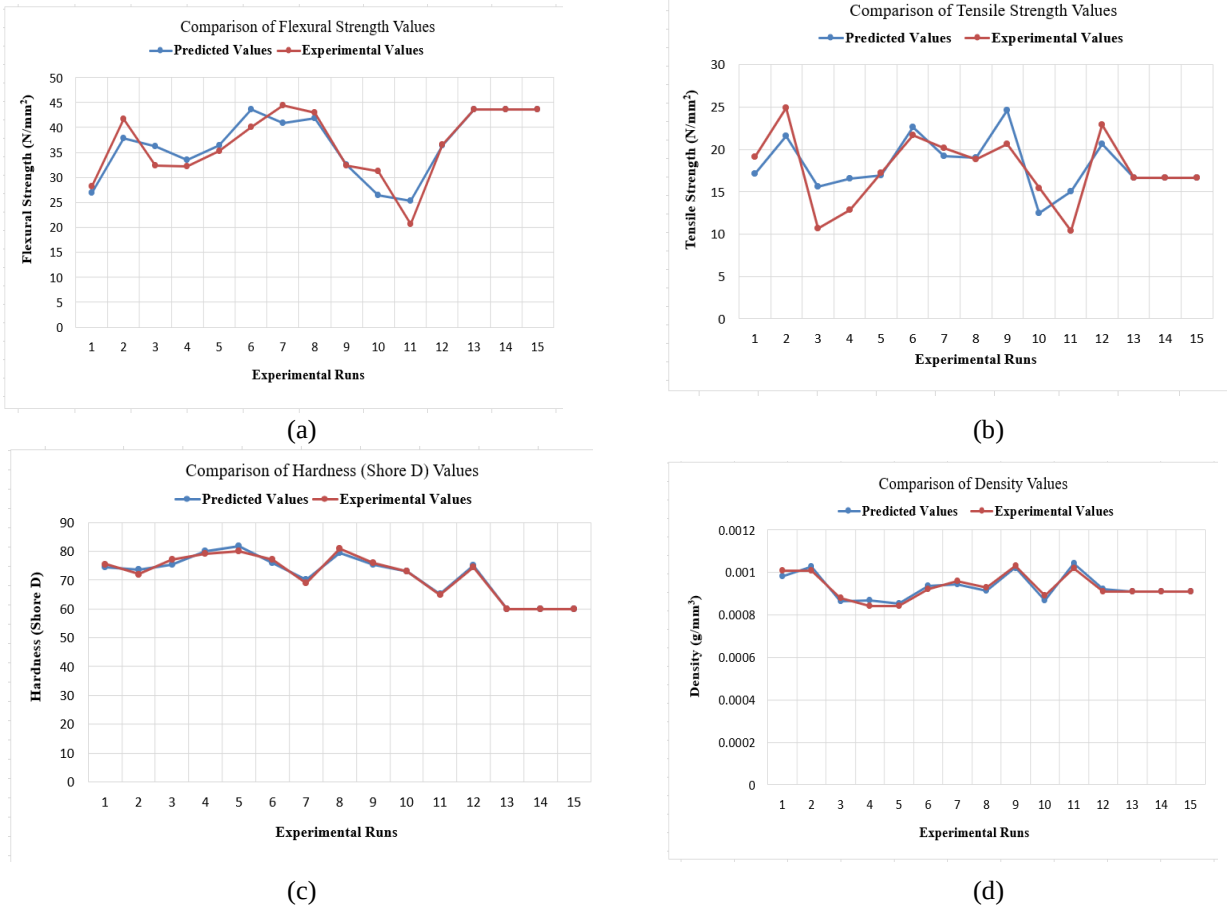

Figure 3. Experimental and predicted values for (a) tensile strength, (b) flexural strength, (c) Hardness and (d) density

(iv) Model accuracy check

To verify the models suitability, residual analysis was used. The normal probability of residuals for: (a) tensile strength, (b) flexural strength, (c) hardness and (d) density is showed in Figure 4. In Figure 4(a) normality assumptions was verified and there is lesser degree of variability in the tensile strength values obtained from the experiments at about 10 points while at some 5 points, range of the degree of variability is about 4.9%. The residuals followed normal distribution and generally fell on the least-square line closely with no large deviations showing an R^2 = 0.9308. The normal probability of residuals for flexural strength (Figure 4(b)) exhibits lesser degree of variability in values obtained from the experiments at about 10 points while at some 5 points, range of the degree of variability is about 4.8%, with an R^2 = 0.9266.The normal probability of residuals for hardness of composites (Figure 4(c)) exhibits negligible variability in the values obtained from the experiments. It followed a normal distribution and fell on the least-square line closely with no reasonable deviations with R^2 = 0.9636.The normal probability of residuals for composite density (Figure 4(d)) exhibits negligible variability in the experimentally obtained values. Hence, the residuals for density followed normal distribution and fell on the least-square line closely with no reasonable deviations with R^2 = 0.9836.

3.3 Property Response surfaces and optimisation

The results of the experimental runs from the BBD in Table 3 were used to obtain the multivariate quadratic models in Table 4 which generally showed good fitness. The independent variables (normalized factors) in these models were defined in equations (2) – (4), while the dependent variables were the properties / parameters measured and recorded. The optimal process values predicted for the mechanical properties from the experiment could be determined by the models for property the response surfaces. The relationships between tensile strength, flexural strength, hardness, and density with the independent process parameters are presented as response surfaces in Figure 5 to Figure 8.

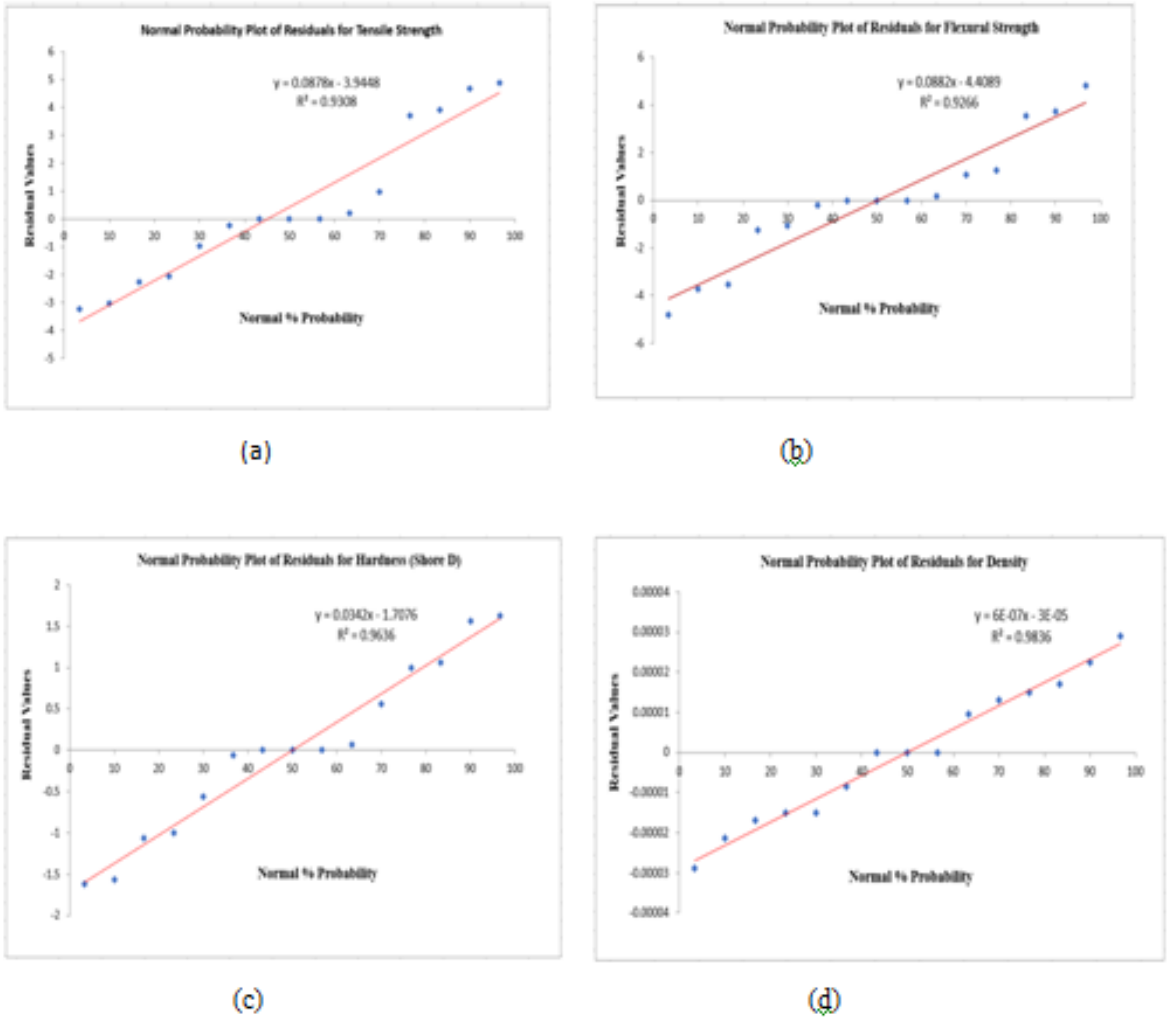

Figure 4. Normal probability of residuals for: (a) tensile strength (b) flexural strength (c) hardness, and (d) density

(i) Hardness Response

The Figure 5 showed a maximum hardness of 89.875SD from 100%CSAC with 60µm particle size at the reinforcement concentration X_W = 4%wt; but 88.625SD from 0%CSAC sample with 150µm at reinforcement concentration X_W = 8%. The minimum hardness of 62.7078SD from 26.67%CSAC with 102µm particle size at the reinforcement concentration X_W = 4%wt; but 67.45778SD from 53.33%CSAC sample with 108µm at reinforcement concentration X_W = 8%wt. This maximum hardness of 88.625SD from 0%CSAC sample with 150µm at reinforcement concentration X_W = 8% is not consistent with other research findings (Ossia & Big-Alabo, 2021; Ossia et al., 2020; Abutu et al., 2019; and Ambali et al., 2019) as hardness had always been known and reported to increase with particle size and not the opposite. Hence, the optimal hardness for reinforcement concentration X_W = 8% is 87.375SD for 100%CSAC with particle size of 60µm instead.

Hardness for reinforcement concentration X_w = 4% and 8% were the same with a hybrid mix of CSAC:PKSAC = 80:20 %Vol giving a value of 82.14SD which was independent of the reinforcement concentration.

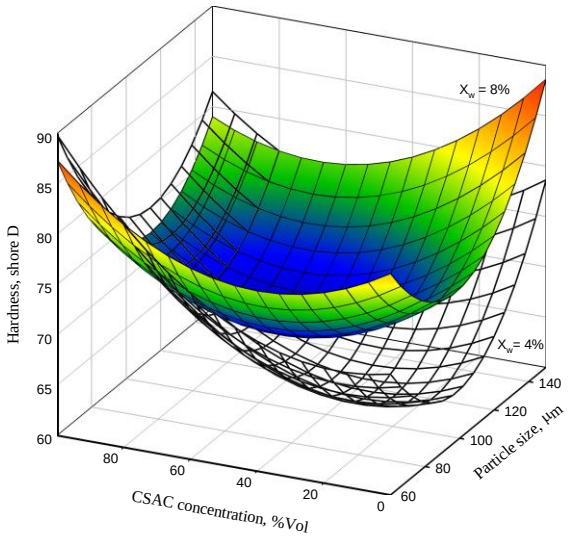

Figure 5. Hardness variation with CSAC, particle size and reinforcement concentration X_W

(ii) Density

From Figure 6, maximum Density D_{max} is 1.0475 occurring with 100% CSAC for 150µm at a weight factor reinforcement X_W = 4%wt but was 0.9425 occurring with 0% CSAC for 60µm at a reinforcement weight factor X_W = 8%wt. The minimum density D_{min} is 0.97 occurring with 100% CSAC for 60µm at a weight factor reinforcement X_W = 4%wt but was 0.8375 occurring with 100% CSAC for 60µm at a reinforcement weight factor X_W = 8%wt. Hence, the optimal density occurs with 100%CSAC at 60µm being 0.97 for reinforcement concentration of 4%, and 100%CSAC at 60µm being 0.8375 for reinforcement concentration of 8%.

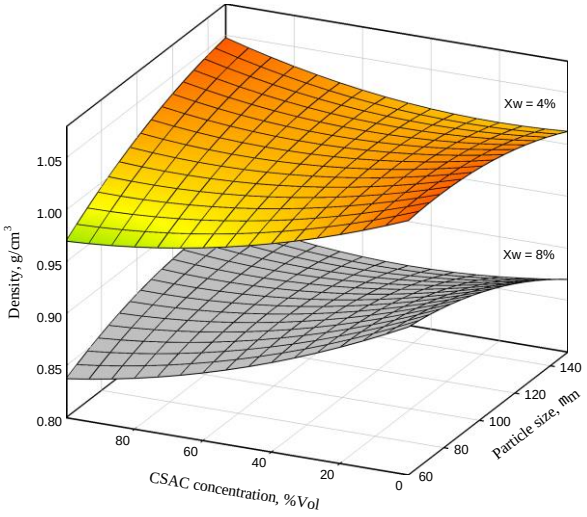

Figure 6. Density variation with CSAC, particle size and reinforcement concentration X_W

(iii) Flexural strength

Figure 7 shows that the maximum flexural strength (SF_{max}) of the friction linings obtained based on the response surfaces was SF_{max} = 39.97696 from 93.33% CSAC of 150µm at reinforcement concentration of X_W = 4%wt; but SF_{max} = 39.4637 from 0% CSAC of 60µm at reinforcement concentration of X_W = 8%wt. Minimum flexural strength (SF_{min}) of the friction linings obtained based on the response surfaces was SF_{min} = 21.7437 from 0% CSAC of 60µm at reinforcement concentration of X_W = 4%wt; but SF_{min} = 26.4118 from 100% CSAC of 84µm at reinforcement concentration of X_W = 8%wt.

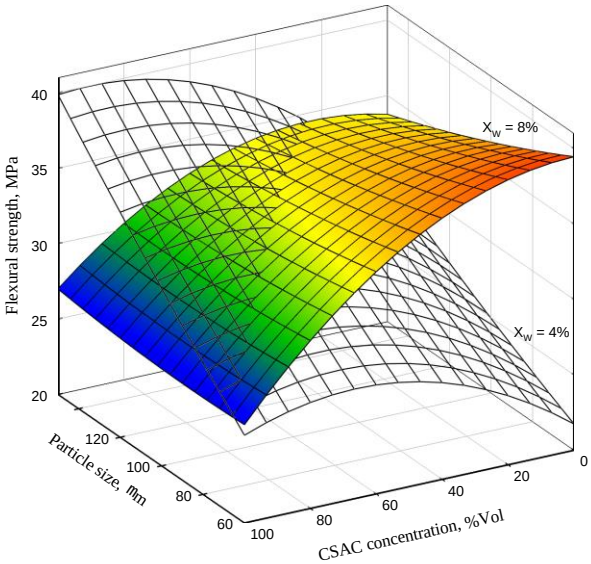

Figure 7. Flexural strength variation with CSAC, particle size and reinforcement concentration X_W

(iv) Tensile strength

The Figure 8 showed a maximum tensile strength (ST_{max}) of 28.65MPa from 100%CSAC with 150µm particle size at the reinforcement concentration X_W = 4%wt; but 21.905MPa from 0%CSAC sample with 60µm at reinforcement concentration X_W = 8%. The minimum tensile strength (ST_{min}) of 14.07528MPa from 0%CSAC with 90µm particle size at the reinforcement concentration X_W = 4%wt; but 10.80624 from 100%CSAC sample with 66µm at reinforcement concentration X_W = 8%wt. From 40%CSAC with particle size of 66µm, the tensile strength (ST) = 15.61814MPa was the same for the reinforcement concentration X_W = 4% and 8%wt.

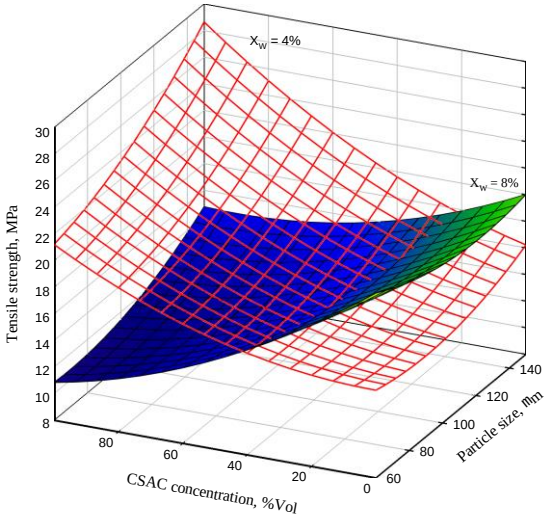

Figure 8. Tensile strength variation with CSAC, particle size and reinforcement concentration X_W

4. CONCLUSION

The physio-mechanical properties of chemically activated agrowaste materials have been optimized as a function of reinforcement particle size X_{PS} (μm), reinforcement weight X_{WT} (%wt) and CSAC concentration X_{CS} (%vol) in composite materials by BBD experiments. Second order multivariate quadratic models (with R^2 = 0.5938, 0.85012, 0.98042 and 0.94189) based on the experimental results were developed to predict physio-mechanical properties (for tensile strength, flexural strength, hardness and density). This implied that these models could be used to predict the values of the properties within the range of the investigated parameters and hence showed good fitness of models. The models are therefore capable of explaining 85%, 98% and 94.2% of the variation in responses, respectively. Results showed negligible variations between the experimental and predicted values of the physic-mechanical properties obtained. The normal probability residuals analysis showed that residuals followed normal distribution and generally fell on the least-square line closely with no large deviations with an R^2 = 0.9308 for tensile strength, R^2 = 0.9266 for flexural strength, R^2 = 0.9636 for hardness, and R^2 = 0.9836 for density of composites. The optimal process parameters were found using 3D response surfaces and optimum mechanical properties were achieved at reinforcement concentration X_W = 8%, 100%CSAC with particle size of 60μm to be 87.375SD for hardness, the optimal density occurs with 100%CSAC at 60μm and reinforcement concentration of 4% being 0.97g/cm^3. The maximum flexural strength (FS_{max}) of the friction linings obtained based on the response surfaces was FS_{max}=39.97696 from 93.33% CSAC of 150μm at reinforcement concentration of X_W=4%wt; whereas the maximum tensile strength TS_{max} of 28.65MPa from 100%CSAC with 150μm particle size at the reinforcement concentration X_{WT} = 4%wt was achieved through the optimized parameters. From this study, it can be observed that the process parameters (reinforcement particle size (X_{PS}) reinforcement weight (X_{WT}) and coconut shell activated carbon (CSAC) concentration (X_{CS})) are important inputs for the fabrication of friction lining composite samples using chemically activated carbon from agro-wastes and greatly influenced their mechanical properties.

REFERENCES

Abutu, J., Lawal, S. A., Ndaliman, M. B., Lafia-Araga, R. A., Adedipe, O., & Choudhury, I. A. (2019). Production and characterization of brake pad developed from coconut, shell reinforcement material using central composite design. *SN Applied Sciences Journal, 1*(82), 1-16. https://doi.org/10.1007/s42452-018-0084-x .

Ambali, I. O., Shuaib-Babata, Y. l., Alasi, T. O., Aremu, I. N., Ibrahim, H. K., Elakhame, Z. U., Abdulraman, S. O. (2019). Suitability of cow horn as filler in an epoxy composite. *Journal of Applied Science & Environmental Management, 23*(3), 475-482. https://dx.doi.org/10.4314/jasem.v23i3.17

Athijayamani, A., Thiruchitrambalam, M., Manikandan, V., & Pazhanivel, B. (2010). Mechanical properties of natural fibres reinforced polyester hybrid composite. *International Journal of Plastics Technology, 14*, 104-116.

Daryoush, E., & Musbah, M. (2011), Comparison of artificial neural network and multiple regression analysis techniques in predicting the mechanical properties of a 356 alloy, *Procedia Engineering, 10*, 589-594.

Hakan, O., & Bulent, M. I. (2017). The mechanical performance of plain and plain derivative woven fabrics reinforced composites: tensile and impact properties. *The Journal of the Textile Institute*, 1-14.

Hughes, M. (2012). Defects in natural fibres: their origin, characteristics and implications for natural fibre-reinforced composites. *Journal of Materials Science, 47*, 599-609.

Latha, B., & Senthilkumar, V. S. (2010). Modelling and analysis of surface roughness parameters in drilling GFRP composites using fuzzy logic. *Materials and Manufacturing Processes, 25*(8), 817-827.

Manickam, C., Kumar, J., Athijayamani, A., & Karthik, K. (2015). Modelling and multi-response optimization of the mechanical properties of roselle fiber-reinforced vinyl ester composite. *Polymer-Plastics Technology and Engineering*, 1-32.

Manikandan, A., Danni, Premkumar, S., & John J. B. (2020). Prediction of Mechanical Properties of Natural Fibers Reinforced Polymer Composites. *Tierärztliche Praxis, 40*, 614-620.

Maniya, K. D., & Bhatt, M. G. (2016). Empirical models for estimating the mechanical and morphological properties of recycled low density polyethylene/snail shell bio-composites. *Journal of the Association of Arab University for Basic and Applied Sciences, 21*, 45-52.

Mustafa, E. U., & Huseyin, K. (2006). Regressional estimation of ring cotton yarn properties from HVI fiber properties', *Textile Research Journal, 76*(5), 360-366.

Nuhu, A. A., & Adeyemi, I. O. (2015). Development and Evaluation of Maize Husks (Asbestos-Free) based Brake *Pad' Industrial Engineering Letters, 5*(2), 74-79.

Ochola, J. R., & Mwasiagi, J. I. (2012). Modelling the influence of cotton fiber properties on ring spun yarn strength using Monte Carlo techniques. *Research & Reviews in Polymer, 3*(3), 84-88.

Oladele, I. O., Balogun, A. O., Adegun, M. H., Obolo, O. E., Agbabiaka, O. G., & Popoola, M. O. (2020). Assessment of the physical, mechanical and wear properties of grass-cutter (thryonomys swinderianus) keratinous hair fiber based polypropylene composites. *Proceedings on Engineering Sciences*, *02*(4) 401-408. doi: 10.24874/PES02.04.007

Ossia C. V., Big-Alabo A., & Ekpruke E. O. (2020). Effect of Particulate Grain Size on the Physicomechanical Properties of Green Automotive Brake Pads from Waste Coconut (*Cocos nucifera L.*) Shells. *Advances in Manufacturing Science & Technology*, *44*(4) 135-144. https://doi.org/10.2478/amst-2019-0023

Ossia, C. V., & Big-Alabo, A. (2021). Development and Characterization of Green Automotive Brake pads from Waste Shells of Giant African Snail *(Achatina achatina L.)*. *International Journal of Advanced Manufacturing Technology, (IJAMT), 114*(9-10), 2887-2897. https://doi.org/10.1007/s00170-021-07085-4

Pandey, J. K., Ahn, S. H., Lee, C. S., Mohanty, A. K., & Mistra, M. (2010). Recent advanced in the application of natural fiber based composites. *Macromolecular Materials and Engineering*, *295*(1), 975-989.

Piyush (2015). Morphological analysis of glass fiber nylon 6 composite. *International Conference on Civil, Materials and Environmental Sciences* (CM, PG, Jitendra, MM & Vijay, PC, 'Modelling of mechanical properties ES), 196-200.

Ruzaidi, C. M., Kamarudin, H., Shamsul, J. B., Abdullah, M. M. A., & Rafiza, (2012). Mechanical properties and wear behaviour of brake pads produced from Palm Slag. *Advanced Materials Research*, 341-341, 26-30.

Singh, S. P. (2015). Analysis of brake pad friction material formulation. *International Journal of Advanced Engineering Research and Science (IJAERS), 2*(8), 6-11.

Yehia, E, M., Broughton, J. R., & Lynch, W. K. (1990). A statistical model for determining the technological value of cotton using HVI fiber properties. *Textile Research Journal*, 495-499.

Leonard M. Akuwueke
Mechanical Engineering Department,
University of Port Harcourt,
Port Harcourt, Nigeria.
leo_akuwueke@yahoo.com

Chinwuba V. Ossia
Mechanical Engineering Department,
University of Port Harcourt,
Port Harcourt, Nigeria.
chinwuba.ossia@uniport.edu.ng

Harold U. Nwosu
Mechanical Engineering Department,
University of Port Harcourt,
Port Harcourt, Nigeria.
Harold.nwosu@uniport.edu.ng